A Computational Model for Estimating Effective Connectivity Using Virtual Neurostimulation

Yanqing Dong[1+](dongyanqing0078@link.tyut.edu.cn), Jing Wei[2+](20141032@sxufe.edu.cn)
Yaru Xu[1](xuyaru0447@link.tyut.edu.cn), Xin Wen[3](xwen@tyut.edu.cn)
Jie Xiang[1*](xiangjie@tyut.edu.cn), Mengni Zhou[3*](zhoumengni@tyut.edu.cn)
[1]College of Computer Science and Technology (College of Data Science), Taiyuan University of Technology
[2]School of Information, Shanxi University of Finance and Economics
[3]School of Software, Taiyuan University of Technology
[+] equal contribution, [*] corresponding author

Abstract

Effective connectivity (EC) is crucial for elucidating causal interactions between brain regions, providing valuable insights into cognitive function. Traditional methods infer EC indirectly through temporal predictions, but unmeasured confounding factors lead to temporal delays, resulting in spurious causal inferences. Compared to the indirect inference of EC using traditional methods, neurostimulation experiments directly infer EC, yet their invasive nature and ethical constraints limit their applicability in assessing whole-brain EC. To address this, we propose a data-theory-driven virtual neurostimulation (VNS) model for directly estimating EC between brain regions. This model constructs a large-scale brain network model as a surrogate for the brain, applying perturbations to specific brain regions based on the physiological mechanism of membrane potential polarization induced by current stimulation. Causal relationships between brain regions are then inferred directly by performing statistical analysis on the responses in blood oxygenation level dependent (BOLD) signals. The model's accuracy and stability were validated on macaque and human medial temporal lobe (MTL) datasets with known ground-truth EC, demonstrating superior performance over baseline methods. Application to a disease-specific dataset further highlights its potential as a personalized biomarker for neurodegenerative diseases, providing a novel pathway for early diagnosis in brain disorders.

Keywords: effective connectivity; causal network; virtual neurostimulation; large-scale brain network model

Introduction

The brain operates as a complex network, collaborating the interactions between multiple brain regions to enable cognitive functions (Park & Friston, 2013). Understanding the information flow and its causal interactions between these regions is crucial for deciphering brain function and facilitating the early diagnosis of neurological disorders (Esmaeil-Zadeh, Fattahi, Soltani-Gol, Rostami, & Soltanian-Zadeh, 2024). Effective connectivity (EC) refers to the neural influence one brain region exerts on another, aiming to clarify the direction of information flow between regions and thereby uncover the dynamic causal interactions within the brain (Schippers, Roebroeck, Renken, Nanetti, & Keysers, 2010).

Numerous methods have been proposed to indirectly estimate EC by analyzing the temporal dynamics of activity across different brain regions. Granger Causal Analysis (GCA) is a widely used causal inference method that infers the causal direction by quantifying the temporal delay between the activities of two variables (Marinazzo, Liao, Chen, & Stramaglia, 2011). Dynamic Causal Modeling (DCM) follows a similar principle of temporal delay but extends it by incorporating the activity of multiple brain regions into a probabilistic graphical model, allowing for different hypotheses to be specified by varying its nodes and directed edges, thereby inferring the causal interactions between brain regions (Friston, Harrison, & Penny, 2003). Although GCA and DCM are widely used for indirect causal inference, they require high temporal precision data. For lower precision techniques, such as functional neuroimaging, unmeasured confounders may introduce temporal delays, heightening the risk of spurious relationships in causal inference (Siddiqi, Kording, Parvizi, & Fox, 2022).

Compared to traditional methods for inferring EC indirectly, neurostimulation experiments (e.g., brain stimulation) provide direct causal inference by observing the effects on brain activity following the perturbation of specific brain regions (Hollunder et al., 2024). However, the "perturbation and recording" process in such experiments faces both ethical and technical challenges, which limit their widespread applicability. To address these limitations, Luo et al. (2025) proposed a data-driven Neural Perturbational Inference (NPI) model. This model utilizes artificial neural networks to simulate perturbations of blood oxygenation level dependent (BOLD) signals in targeted brain regions and track the resulting responses in BOLD signals across other regions, thereby inferring EC between brain regions. However, the approach relies on large amounts of high-quality data to train robust neural networks, and the black-box nature of these networks diminishes their biological interpretability, hindering the ability to provide mechanistic insights.

In this work, we propose a novel approach for modeling EC based on a virtual neurostimulation (VNS) model, which utilizes a biophysical large-scale brain network model that accurately represents neural activity in the brain (Al-Hossenat, Song, Wen, & Li, 2022; Castaldo et al., 2023; Lu et al., 2024). Specifically, we implement a large-scale brain network model as a surrogate for the brain, applying virtual perturbations based on the membrane potential polarization mechanisms triggered by current stimulation (Kunze, Hunold, Haueisen, Jirsa, & Spiegler, 2016; Nitsche & Paulus, 2000). By observing the BOLD signal responses in the rest of regions and applying statistical tests, we further infer the causal interactions between brain regions. The VNS model effectively overcomes the ethical and technical limitations inherent in

In D. Barner, N.R. Bramley, A. Ruggeri and C.M. Walker (Eds.), *Proceedings of the 47th Annual Conference of the Cognitive Science Society*

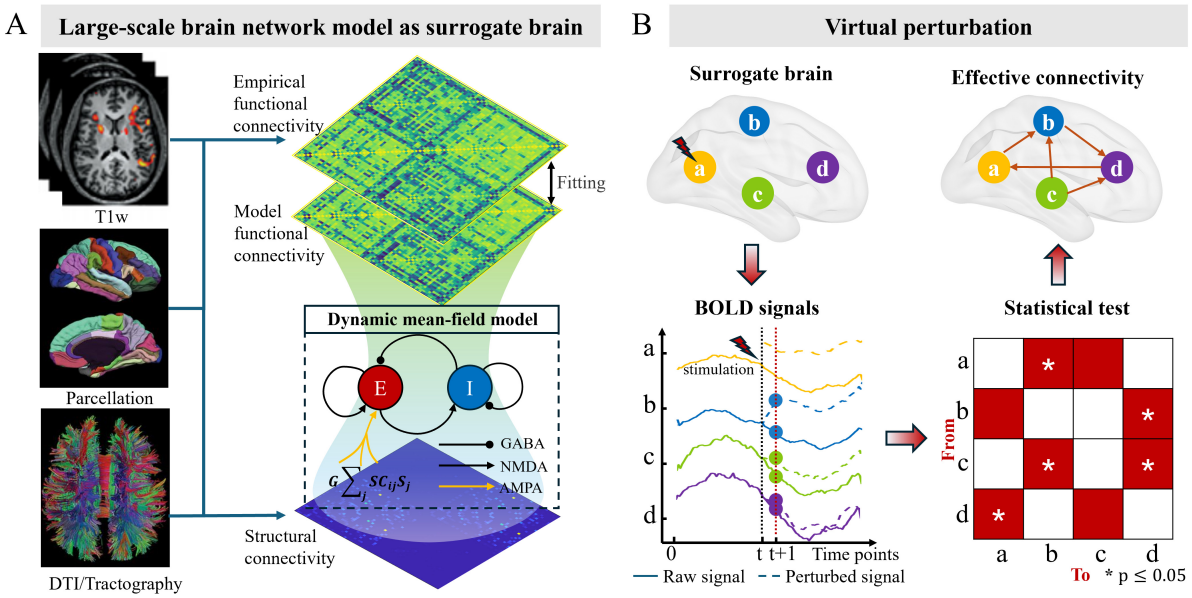

Figure 1: Virtual neurostimulation (VNS) model. (A) Constructing a large-scale brain network model as a surrogate for the complex dynamics of the real brain. (B) A virtual perturbation is applied to brain region a in the surrogate brain model (top-left of the figure). By analyzing the resulting fluctuations in the BOLD signal responses of other brain regions, the effective connectivity (EC) from region a to other regions is directly inferred (bottom-left). Next, perturbations are applied sequentially to each brain region to derive the full brain's directed connectivity, followed by statistical testing (bottom-right), which ultimately yields the final full-brain EC (top-right).

traditional neurostimulation experiments and offers a novel perspective for analyzing brain causal networks.

Methods

We propose a virtual neurostimulation (VNS) model to non-invasively infer EC between brain regions from BOLD signals, as illustrated in Figure 1. We modeled a surrogate brain based on a large-scale brain network to simulate neural activity within the brain (Figure 1A). Drawing on the physiological mechanisms underlying brain activity induced by current stimulation, we apply virtual perturbations to individual brain regions. By observing the dynamic responses in BOLD signals from other brain regions, we further infer the causal network within the brain (Figure 1B). The VNS effectively captures causal interactions between brain regions by analyzing responses in brain activity induced by virtual perturbations.

Large-scale brain network model as surrogate brain

We modeled a large-scale brain network model consisting of multiple neural masses to simulate dynamic brain activity. The neural mass model employs the dynamic mean-field model (MFM), proposed by Deco et al. (2013), which captures the dynamics of local cortical regions. The coupling between cortical regions is determined by structural connectivity. The MFM was derived by applying mean-field reductions to a spiking neural network model, which incorporates firing rates and synaptic gating dynamics (Wong-Lin & Wang, 2006). Each cortical region was represented by subnetworks of coupled excitatory and inhibitory populations of spiking neurons, described by the following set of nonlinear stochastic differential equations:

$$\dot{S}_i = -\frac{S_i}{\tau_S} + \gamma(1 - S_i)H(x_i) + \sigma\xi_i(t) \tag{1}$$

$$x_i = wJS_i + GJ\sum_j C_{ij}S_j + I \tag{2}$$

$$H(x_i) = \frac{ax_i - b}{1 - \exp(-d(ax_i - b))} \tag{3}$$

Where $\dot{S}_i$, x_i, and $H(x_i)$ denote the average synaptic gating variable, the total input current, and the average firing rate of each population in the cortical region i, respectively. The neuronal population firing rate $H(x_i)$ depends on the total input current x_i. The parameters are derived from values extracted from neurophysiological data to ensure the biophysical realism of the model (Gordon et al., 2017). A detailed definition of these parameters and the procedure for fitting large-scale dynamic models are provided in previous work (Wei et al., 2022). Using the dynamic MFM, we can construct a surrogate brain that effectively replicates the complex and realistic dynamic activity of the brain.

Virtual perturbation

Once the large-scale brain network model is trained, we perform virtual perturbations on each brain region to infer EC between regions. Specifically, based on the physiological mechanisms underlying membrane potential changes induced by current stimulation, we perturb the average synaptic gating variable in the surrogate brain model, as shown in Equation 4.

$$\dot{S'}_i = -\frac{S_i}{\tau_S} + \gamma(1 - S_i)H(x_i) + \sigma\xi_i(t) + \delta(i,t) \quad (4)$$

Here, $\dot{S'}_i$ represents the average synaptic gating variable after the perturbation, and $\delta(i,t)$ denotes the intensity of the stimulation applied to brain region i at time t. Each perturbation targets a single brain region at a time, while the signals from all other regions remain unchanged. Due to the sensitivity of the brain's response to perturbations with respect to its initial state, we performed multiple simulations for each perturbation to mitigate the influence of this variability (Luo et al., 2025).

By applying virtual perturbations to brain region i and observing the BOLD signal response activity in brain region j, the effective connectivity from region i to region j is defined as:

$$EC_{ij} = E_{t+1}\left[B'_{ij}(t+1) - B_{ij}(t+1)\right] \bullet \mathbb{1}(p_{ij} \leq 0.05) \quad (5)$$

When region i is perturbed, the BOLD signal of region j is denoted as B'_{ij}; while in the absence of perturbation to region i, the BOLD signal of region j is denoted as B_{ij}. p_{ij} represents the p-value obtained from a paired sample t-test between the 30 simulated values of B'_{ij} and B_{ij}, which is subsequently corrected for multiple comparisons using the False Discovery Rate (FDR) method. The indicator function $\mathbb{1}(p_{ij} \leq 0.05)$ takes a value of 1 if $p_{ij} \leq 0.05$, indicating the presence of EC from region i to region j; otherwise, the connection is considered invalid. E represents the average response from applying perturbations across 30 simulations, with the averaged response used as the final EC.

Datasets

To validate the effectiveness of the VNS model, we conducted evaluations using three publicly available datasets. First, we utilized synthetic data from macaques, which includes ground-truth EC, to assess the accuracy of the VNS model in inferring EC. Second, we applied a real fMRI data from the human medial temporal lobe (MTL), with ground-truth EC as reported in previous studies (Sanchez-Romero et al., 2019), to further evaluate the model's ability to infer EC in the human brain. Finally, we employed the Alzheimer's Disease Neuroimaging Initiative (ADNI) dataset to assess the sensitivity of EC inferred by VNS in capturing disease-specific changes.

Synthetic Data from Macaques. We utilized a publicly available synthetic dataset derived from macaques, which can be accessed at: `http://github.com/cabal-cmu/Feedback-Discovery`. Sanchez-Romero et al. (2019) partitioned the entire macaque network into distinct subnetworks at different scales based on their structural connectivity characteristics, including SmallDegree (SD, 28 nodes), LongRange (LR, 67 nodes), and Full (91 nodes). They further simulated BOLD signals based on these macaque brain networks, generating 60 distinct individual data, each containing 500 time points.

Real fMRI Data from the Human MTL. We utilized a publicly available high-resolution 7T resting-state functional magnetic resonance imaging (rs-fMRI) dataset sourced from the human medial temporal lobe (MTL), available at `https://github.com/shahpreya/MTLnet`. The dataset includes rs-fMRI data from 23 subjects, acquired with TR = 1 s, providing 421 time points per subject. It includes seven regions of interest within the MTL of both left and right hemispheres.

Alzheimer's Disease Dataset. We applied the VNS model to the ADNI dataset (`http://adni.loni.usc.edu/`), which includes subjects with Alzheimer's disease (AD, n=21), mild cognitive impairment (MCI, n=33), and normal control (NC, n=29). These participants underwent multimodal imaging, including rs-fMRI, T1-weighted imaging, and diffusion tensor imaging (DTI). All rs-fMRI data were acquired using a 3T MRI scanner with TR = 3 s, providing 187 time points per subject. For the rs-fMRI data, the brain was parcellated into 68 regions based on the Desikan-Killiany brain atlas.

Evaluation Metrics

To assess the performance of the inferred EC method, we computed a range of metrics, including accuracy (ACC), precision (PRE), sensitivity (SEN), and specificity (SPE).

$$Precision = \frac{TP}{TP+FP} \quad (6)$$

$$Accuracy = \frac{TP+TN}{TP+TN+FP+FN} \quad (7)$$

$$Sensitivity = \frac{TP}{TP+FN} \quad (8)$$

$$Specificity = \frac{TN}{TN+FP} \quad (9)$$

Here, true positive (TP) refers to edges present in both the estimated and true EC; false positive (FP) refers to edges present in the estimated EC but absent in the true EC; false negative (FN) refers to edges present in the true EC but absent in the estimated EC; and true negative (TN) refers to edges are absent in both the true and estimated EC.

Results

To validate our model's ability to infer causal interactions between brain regions, we employed two baseline methods:(1) GCA, an indirect causal inference approach based on time series prediction. Considering that DCM relies on specific

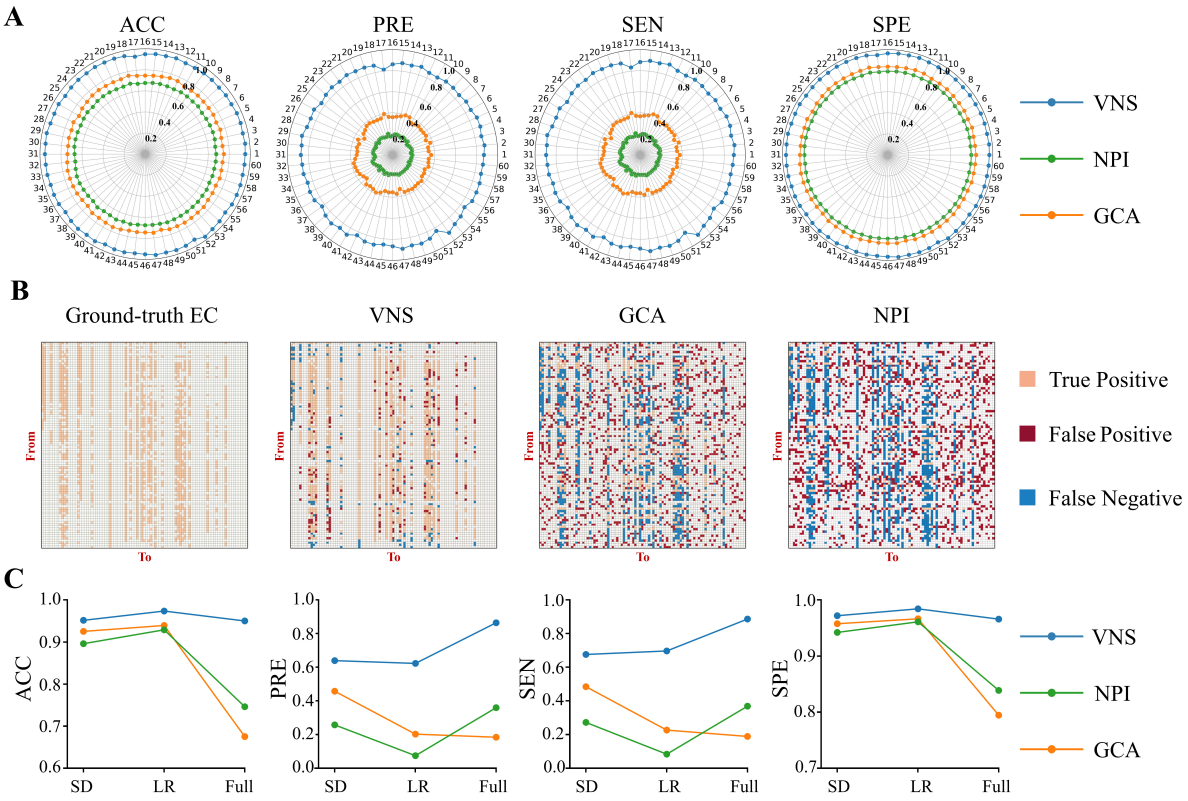

Figure 2: Results of synthetic dataset from macaques. (A) Comparison of EC inference performance for each subject in the Full network, with the outer numbers representing the subjects. (B) EC from a randomly selected subject in the macaque Full network. (C) Comparison of the average EC inference performance across networks at different scales (SD, LR, and Full).

model assumptions, which may lead to biases due to model mismatch, we chose GCA as the baseline method. (2) NPI, which directly estimates EC. These baseline methods were used for comparison with our model, allowing for a comprehensive evaluation of its performance and accuracy in causal inference.

Results on Macaque synthetic Dataset

To evaluate the accuracy of VNS in inferring EC, we conducted validation using a synthetic dataset from macaques (Figure 2). We conducted a comprehensive evaluation of the accuracy and generalization performance of three methods for inferring EC within the Full subnetwork, encompassing 60 macaques (Figure 2A). The results demonstrate that the VNS outperforms the baseline methods across all subjects, exhibiting remarkable cross-subject generalization capabilities. Then, we randomly selected a subject from the macaque Full subnetwork and compared the EC inferred by three different methods with their ground-truth EC (Figure 2B). The results indicate that VNS more accurately captures the true neural connectivity pattern, whereas both GCA and NPI exhibited a higher frequency of misjudgments during causal inference, including spurious connections (false positive) and missed true connections (false negative). Finally, we compared the average performance of the three methods across different network scales, including small-scale networks SD, medium-scale networks LR, and full-scale networks Full (Figure 2C). The results exhibit that the VNS consistently outperforms the baseline methods across all network scales, with its relative advantage becoming increasingly pronounced as the network scale expands. The exceptional performance on the macaque synthetic dataset further validates the accuracy, generalization, and robustness of the VNS in inferring EC.

Results on Real Human MTL fMRI Dataset

To further validate the applicability of the VNS model in accurately inferring causal relationships within the human brain, we applied it to real fMRI dataset from the MTL of both the left and right hemispheres. Building on previous studies, we defined the criterion for EC (Sanchez-Romero et al., 2019; Zhang, Zhang, Ji, & Liu, 2023): a connection was considered effective if it was consistently observed in at least 45% of the subjects; otherwise, it was deemed ineffective. Notably, although a gold standard for evaluating the performance of causal search algorithms in the human brain remains absent, prior research has provided support for 'ground-truth EC' in the causal interactions between regions

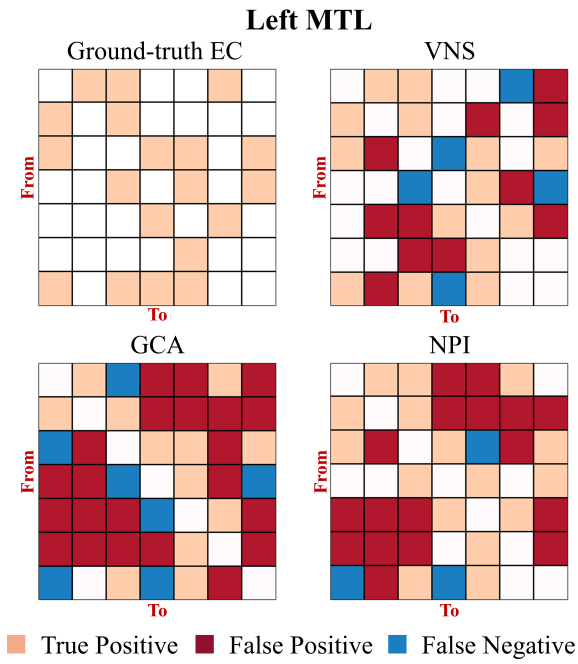

Figure 3: EC of the left MTL in the human brain.

of the MTL (Sanchez-Romero et al., 2019).

We applied three methods to analyze the dataset from the left MTL of the human brain, revealing the EC patterns between regions within the MTL (Figure 3). The results show that the VNS outperforms the baseline methods in reducing both FP and FN, thereby enabling a more accurate reconstruction of the ground-truth EC structure. Additionally, we evaluated the performance of the three methods using metrics such as ACC, PRE, SEN, and SPE (Table 1). The results indicate that VNS significantly outperforms the baseline methods in terms of ACC, PRE, and SPE, highlighting its superior reliability and robustness. Although the NPI method exhibits superior SEN, its higher FP rate reflects the identification of numerous spurious connections, leading to a misleading increase in SEN.

Table 1: Comparison of the performance in inferred EC on the human MTL dataset.

Task	Method	ACC	PRE	SEN	SPE
Left MTL	GCA	0.310	0.360	0.632	0.044
	NPI	0.524	0.485	**0.842**	0.261
	VNS	**0.620**	**0.560**	0.747	**0.522**
Right MTL	GCA	0.405	0.400	0.778	0.130
	NPI	0.548	0.487	**1.000**	0.210
	VNS	**0.600**	**0.520**	0.722	**0.500**

Results on the ADNI Dataset

To explore the potential of VNS-inferred EC as a biomarker, we applied the VNS model on the ADNI dataset to construct individual EC networks (Figure 4A). We performed 1000 permutation tests to analyze the significant differences in EC among patients with AD, MCI, and NC, applying a FDR correction to control for false positives in the multiple comparison process. These significant connectivity differences (Figure 4B) primarily involve the information transfer from the left temporal lobe and occipital regions to the right parahippocampal gyrus and temporal pole. Structural and functional abnormalities in these regions have been consistently observed and are closely associated with the characteristic cognitive impairments of AD, such as memory decline and impaired spatial orientation (Imai, Matsuoka, & Narumoto, 2023; Tang et al., 2024). Particularly, the parahippocampal gyrus and temporal pole play crucial roles in memory recognition, emotional regulation, and spatial navigation (Hung, Wang, Wang, & Bi, 2020; Riegel et al., 2022).

To further analyze the intergroup differences, we performed independent samples t-tests on the differential connections identified previously (Figure 4C). Compared to the NC, the AD group exhibited significant increases in the connectivity strength of 11 connections ($p \leq 0.05$). The MCI group showed increased connectivity only from L.CUN to R.paraH and from L.periCAL to R.paraH ($p \leq 0.05$). The observed enhancement in connectivity is consistent with existing research and may reflect compensatory mechanisms in AD (Larsen et al., 2021; Power, Venkatesan, Qu, Mclaurin, & Lambe, 2024). Specifically, during the early stages of pathological changes, the brain may strengthen connections between specific regions, particularly those involved in memory and emotional regulation, due to the compensatory reallocation of cognitive resources. These findings provide potential biomarkers for the early diagnosis of AD.

Table 2: Comparison of average classification performance on the ADNI dataset.

Task	Method	ACC	PRE	SEN	SPE
AD vs. NC	GCA	0.860	0.834	0.845	0.854
	NPI	0.880	0.836	0.710	0.862
	VNS	**0.920**	**0.937**	**0.883**	**0.955**
AD vs. MCI	GCA	0.820	**0.903**	0.769	0.853
	NPI	0.853	0.892	**0.938**	0.820
	VNS	**0.871**	0.895	0.901	**0.928**
MCI vs. NC	GCA	0.683	0.706	0.643	0.647
	NPI	0.695	0.741	0.567	0.718
	VNS	**0.710**	**0.770**	**0.715**	**0.733**

As the ADNI dataset lacks a ground-truth EC, we conducted a classification experiment to further evaluate the performance of the VNS in comparison to baseline methods (Table 2). If a method can accurately estimate the EC between brain regions, it is considered to capture disease-specific char-

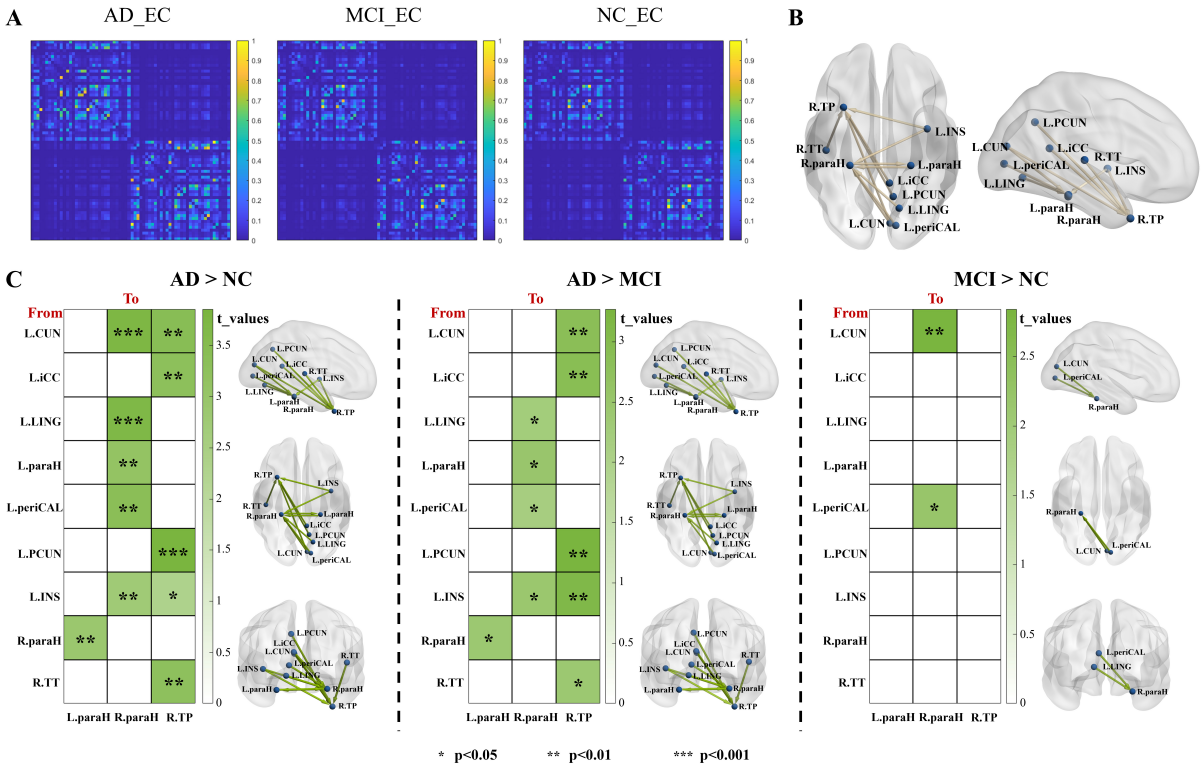

Figure 4: Results of ADNI dataset. (A) Inferred EC of AD, MCI, and NC using VNS. (B) Significant differences in EC between AD, MCI, and NC groups. (C) EC with significant differences between the two groups.

acteristics and exhibit high classification performance (Ji, Liu, Han, & Wang, 2021). Specifically, we utilized the EC as features and employed the Minimum Redundancy Maximum Relevance (MRMR) method for feature selection, retaining the top 100 most informative features. Subsequently, we performed classification using a Support Vector Machine (SVM) model with a linear kernel. The model's hyperparameters were optimized through Bayesian Optimization, with a maximum of 1000 iterations for the optimization process. All experiments were conducted using five-fold cross-validation to ensure the robustness of the results. The results show that the average classification accuracy of the VNS outperforms both the GCA and NPI methods, highlighting the superior reliability and accuracy of the VNS model in estimating EC.

Discussion

In this work, we proposed a data-theory-driven VNS model aimed at accurately inferring whole-brain EC and revealing causal interactions between brain regions. Unlike traditional indirect inference methods, the VNS directly estimates EC from the dynamic response of BOLD signals by simulating the application of current stimulation to specific brain regions. We comprehensively evaluated the effectiveness of the VNS model by comparing it with baseline methods, including GCA and NPI. First, using a gold-standard synthetic dataset from macaques, the VNS model showed high accuracy and stability in inferring EC, significantly outperforming the baseline methods, thereby validating its ability to infer causal relationships between brain regions. Second, experiments using a real fMRI dataset from the human medial temporal lobe (MTL) further validated that the VNS model can accurately infer causal interactions between brain regions, establishing it as an effective tool for exploring inter-regional causal mechanisms in the human brain. Finally, we applied the VNS to the ADNI dataset, revealing significant changes in the EC of AD patients, particularly in brain regions closely associated with memory and emotional regulation, such as the parahippocampal gyrus and temporal pole. Compared to NC, the enhanced abnormal connectivity observed in AD and MCI patients may reflect disruptions in functional networks and potential compensatory mechanisms during disease progression. These findings are consistent with prior literature, further supporting the potential of EC inferred by VNS as a biomarker for brain disorders. In conclusion, we provide comprehensive validation of the VNS model's potential for inferring EC and analyzing causal relationships. By offering a novel, non-invasive approach, the VNS model not only effectively mitigates the risks associated with invasive neurostimulation experiments but also provides valuable insights into the pathological mechanisms underlying brain disorders.

Acknowledgments

This work was supported by the following grants: the National Natural Science Foundation of China 62376184 (Jie Xiang), 62303445 (Mengni Zhou), and 62206196 (Xin Wen), Central Guided Local Science and Technology Development Project YDZJSX20231A017 (Jie Xiang), Shanxi Provincial Application Basic Research Plan 202303021212166 (Jing Wei), Shenzhen Science and Technology Program JCYJ20230807140719040 (Mengni Zhou).

References

Al-Hossenat, A., Song, B., Wen, P., & Li, Y. (2022). Novel large scale brain network models for eeg epileptic pattern generations. *Expert Systems with Applications*, *194*, 116477.

Castaldo, F., Páscoa dos Santos, F., Timms, R. C., Cabral, J., Vohryzek, J., Deco, G., ... Litvak, V. (2023). Multimodal and multi-model interrogation of large-scale functional brain networks. *NeuroImage*, *277*, 120236.

Deco, G., Ponce-Alvarez, A., Mantini, D., Romani, G. L., Hagmann, P., & Corbetta, M. (2013). Resting-state functional connectivity emerges from structurally and dynamically shaped slow linear fluctuations. *Journal of Neuroscience*, *33*(27), 11239–11252.

Esmaeil-Zadeh, M., Fattahi, M., Soltani-Gol, M., Rostami, R., & Soltanian-Zadeh, H. (2024). Effective connectivity estimation by a hybrid neural network, empirical wavelet transform, and bayesian optimization. *IEEE Journal of Biomedical and Health Informatics*, *28*(10), 5696–5707.

Friston, K., Harrison, L., & Penny, W. (2003). Dynamic causal modelling. *NeuroImage*, *19*(4), 1273–1302.

Gordon, E. M., Laumann, T. O., Gilmore, A. W., Newbold, D. J., Greene, D. J., Berg, J. J., ... Dosenbach, N. U. (2017). Precision functional mapping of individual human brains. *Neuron*, *95*(4), 791–807.e7.

Hollunder, B., Ostrem, J. L., Sahin, I. A., Rajamani, N., Oxenford, S., Butenko, K., ... Horn, A. (2024). Mapping dysfunctional circuits in the frontal cortex using deep brain stimulation. *Nature Neuroscience*, *27*(3), 573–586.

Hung, J., Wang, X., Wang, X., & Bi, Y. (2020). Functional subdivisions in the anterior temporal lobes: a large scale meta-analytic investigation. *Neuroscience and Biobehavioral Reviews*, *115*, 134–145.

Imai, A., Matsuoka, T., & Narumoto, J. (2023). Emotional dysregulation in mild behavioral impairment is associated with reduced cortical thickness in the right supramarginal gyrus. *Journal of Alzheimers Disease*, *93*(2), 521–532.

Ji, J., Liu, J., Han, L., & Wang, F. (2021). Estimating effective connectivity by recurrent generative adversarial networks. *IEEE Transactions on Medical Imaging*, *40*(12), 3326–3336.

Kunze, T., Hunold, A., Haueisen, J., Jirsa, V., & Spiegler, A. (2016). Transcranial direct current stimulation changes resting state functional connectivity: A large-scale brain network modeling study. *NeuroImage*, *140*, 174–187.

Larsen, E., Oh, J. Y., Mladinov, M., Lew, C., Li, S., Neylan, T., ... Grinberg, L. T. (2021). Degeneration of human orexinergic neurons across braak stages of alzheimer's disease: Implication for pathogenesis, sleep dysfunction, and therapy. *Alzheimers and Dementia*, *17*(S3), e052465.

Lu, W., Zeng, L., Wang, J., Xiang, S., Qi, Y., Zheng, Q., ... Feng, J. (2024). Imitating and exploring the human brain's resting and task-performing states via brain computing: scaling and architecture. *National Science Review*, *11*(5), nwae080.

Luo, Z., Peng, K., Liang, Z., Cai, S., Xu, C., Li, D., ... Liu, Q. (2025). Mapping effective connectivity by virtually perturbing a surrogate brain. *Nature Methods*.

Marinazzo, D., Liao, W., Chen, H., & Stramaglia, S. (2011). Nonlinear connectivity by granger causality. *NeuroImage*, *58*(2), 330–338.

Nitsche, M. A., & Paulus, W. (2000). Excitability changes induced in the human motor cortex by weak transcranial direct current stimulation. *the Journal of Physiology*, *527*, 633–639.

Park, H.-J., & Friston, K. (2013). Structural and functional brain networks: From connections to cognition. *Science*, *342*(6158), 1238411.

Power, S. K., Venkatesan, S., Qu, S., Mclaurin, J., & Lambe, E. K. (2024). Enhanced prefrontal nicotinic signaling as evidence of active compensation in alzheimer's disease models. *Translational Neurodegeneration*, *13*(1), 58.

Riegel, M., Wierzba, M., Wypych, M., Ritchey, M., Jednoróg, K., Grabowska, A., ... Marchewka, A. (2022). Distinct medial-temporal lobe mechanisms of encoding and amygdala-mediated memory reinstatement for disgust and fear. *NeuroImage*, *251*, 118889.

Sanchez-Romero, R., Ramsey, J. D., Zhang, K., Glymour, M. R. K., Huang, B., & Glymour, C. (2019). Estimating feedforward and feedback effective connections from fmri time series: Assessments of statistical methods. *Network Neuroscience*, *3*(2), 274–306.

Schippers, M. B., Roebroeck, A., Renken, R., Nanetti, L., & Keysers, C. (2010). Mapping the information flow from one brain to another during gestural communication. *Proceedings of the National Academy of Sciences*, *107*(20), 9388–9393.

Siddiqi, S. H., Kording, K. P., Parvizi, J., & Fox, M. D. (2022). Causal mapping of human brain function. *Nature Reviews Neuroscience*, *23*, 361–375.

Tang, X., Guo, Z., Chen, G., Sun, S., Xiao, S., Chen, P., ... Wang, Y. (2024). A multimodal meta-analytical evidence of functional and structural brain abnormalities across alzheimer's disease spectrum. *Ageing Research Reviews*, *95*, 102240.

Wei, J., Wang, B., Yang, Y., Niu, Y., Yang, L., Guo, Y., & Xiang, J. (2022). Effects of virtual lesions on temporal dynamics in cortical networks based on personalized dynamic models. *NeuroImage*, *254*, 119087.

Wong-Lin, K., & Wang, X.-J. (2006). A recurrent network

mechanism of time integration in perceptual decisions. *the Journal of Neuroscience*, *26*, 1314–1328.

Zhang, Z., Zhang, Z., Ji, J., & Liu, J. (2023). Amortization transformer for brain effective connectivity estimation from fmri data. *Brain Sciences*, *13*(7), 995.